

Microwave surface impedance of $\text{YBa}_2\text{Cu}_3\text{O}_{6.99}$: Comparison of theory and experiment

Herman J. Fink

Department of Electrical and Computer Engineering, University of California, Davis, California 95616

(Received 20 April 1999)

Surface resistance experiments by the Vancouver group on very high quality single crystals of $\text{YBa}_2\text{Cu}_3\text{O}_{6.99}$ are compared with a model proposed by Trunin *et al.* and the author. The resistance measurements are from 1.14 to 75.3 GHz, and good numerical agreement is found over that frequency interval for all temperatures. From these measurements the real part of the microwave conductivity $\sigma'(T)$ was extracted, and from it a Drude-like conductivity spectrum was obtained below 25 K, all in agreement with the model. From the conductivity spectrum the scattering rate of the thermally excited quasiparticles was found to increase with temperature (T), in agreement with a Grüneisen T dependent intrinsic resistivity at low temperatures.

Understanding microwave losses in cuprate superconductors is important in advancing a unified picture of high- T_c superconductors. Many experiments¹⁻¹⁸ have been performed on $\text{YBa}_2\text{Cu}_3\text{O}_{7-\delta}$ as the quality and purity of the crystals has been evolving over the years. Films used recently by Hensen, Rieck and co-workers^{19,20} and crystals by the Vancouver group²¹ appear to be of the highest quality. We shall make a comparison of the latest experiments²¹ on $\text{YBa}_2\text{Cu}_3\text{O}_{6.99}$ (YBCO) with a model proposed by Trunin *et al.*¹⁶ and the author.²² It should, however, be remembered that other authors have introduced and studied d -wave pairing,²³⁻²⁶ anisotropic s -wave mechanisms,²⁷ proximity coupling between superconducting CuO_2 planes with every other layer normal,²⁸ a nested Fermi-liquid surface,²⁹ an energy gap,³⁰ and two-fluid models³¹ and their consequences on the microwave conductivity $\sigma = \sigma' - i\sigma''$. They found reasonable success in describing the data of the surface resistance $R_s(\omega, T)$ and of the penetration depth $\lambda(T)$, over moderate temperature and frequency intervals ($\omega = 2\pi f$).

Measurements show that the penetration depth $\lambda(T)$ of high quality crystals of $\text{YBa}_2\text{Cu}_3\text{O}_{7-\delta}$ has a predominantly linear temperature dependence in the ab plane at low temperatures. Crystals of lesser qualities do not show the same temperature dependence at low temperatures. It is interesting to note that $\text{YBa}_2\text{Cu}_3\text{O}_{7-\delta}$ is anisotropic. Measurements^{9,10} with currents flowing parallel to the a , b , and c directions are described by different parameters $\lambda(0)$, $\sigma_{dc}(T_c)$, etc. Measurements of the surface resistance R_s in the ab plane with currents along the a direction²¹ at 1.14, 2.25, 13.4, 22.7, and 75.3 GHz show also a linear temperature dependence at low temperatures. The extrapolated resistance R_0 to 0 K seems to be small for frequencies below 22.7 GHz for the Vancouver crystals²¹ and is neglected in the present investigations. The author estimates R_0 to be smaller than or approximately equal to $10^{-25} \times f^2 \Omega$. Although explicit microscopic calculations²⁵⁻²⁹ have been published which contain many of the qualitative features which are reported here, we shall show to what extent the microwave surface resistance measurements are compatible with the paradigm of Trunin *et al.*¹⁶ and the author.²²

The real part of the surface impedance $\text{Re}[Z_s] = R_s$ is a measure of the microwave power absorbed. With the definition $s \equiv (\sigma'/\sigma'')^2$ the real and imaginary parts of Z_s are

$$R_s = \sqrt{\frac{\omega\mu_0}{2\sigma''}} \sqrt{\frac{\sqrt{1+s}-1}{1+s}}, \quad (1)$$

$$X_s = \sqrt{\frac{\omega\mu_0}{2\sigma''}} \sqrt{\frac{\sqrt{1+s}+1}{1+s}}. \quad (2)$$

Below T_c the density of the quasiparticles $n_n(t)$ decreases while the superelectron density $n_s(t)$ increases, conserving the total number of electrons n :

$$\frac{n_n(t)}{n} = 1 - \frac{n_s(t)}{n} = 1 - \left(\frac{\lambda(0)}{\lambda(t)} \right)^2, \quad (3)$$

where $t = T/T_c$ and $\lambda^2(t) = m/\mu_0 e^2 n_s(t)$.

In the normal state, just above T_c , the conductivity is

$$\sigma = \sigma' - i\sigma'' = \sigma_{dc} \frac{1 - i\omega\tau}{1 + (\omega\tau)^2}. \quad (4)$$

By Matthiessen's rule, the resistivity of a metal at low temperatures consists of two terms: (1) the residual, which is due to electron scattering by impurities, and (2) the intrinsic, which depends on the thermal motion of the lattice and is limited to small angle scattering of the electrons. We apply Matthiessen's rule to $\text{YBa}_2\text{Cu}_3\text{O}_{7-\delta}$. The first term is temperature independent.³² The second term is a function of temperature and is governed at all temperatures by the Grüneisen formula³³ $\rho_i \propto TG(\Theta_D/T)$, where Θ_D is the Debye temperature and

$$G(\Theta_D/T) = (\Theta_D/T)^{-4} \int_0^{\Theta_D/T} \frac{x^5 dx}{(e^x - 1)(1 - e^{-x})}. \quad (5)$$

Thus, we write for the resistivity

$$\rho_{dc}(t) = \rho_r + \rho_i(1)t^5 g(t), \quad (6)$$

where

$$g(t) = f\left(\frac{\Theta_D}{T_c} \frac{1}{t}\right) / f\left(\frac{\Theta_D}{T_c}\right), \quad (7)$$

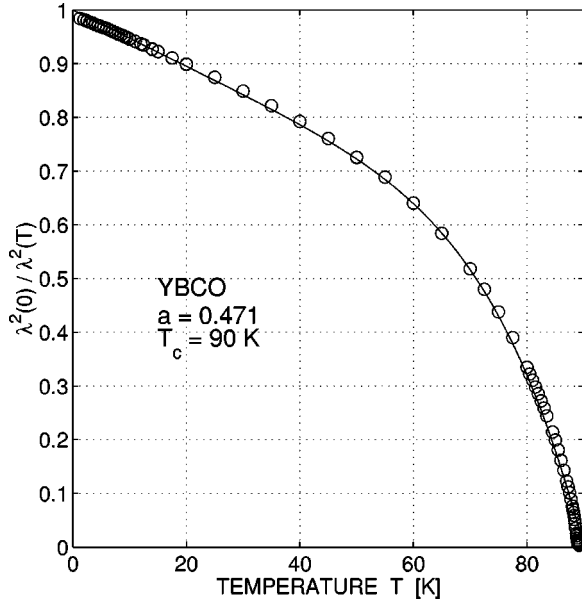


FIG. 1. Plot of Eq. (13) showing the fit to the empirical $[\lambda(0)/\lambda(t)]^2$ as a function of temperature. The experimental points are from Ref. 21, Fig. 3.

with $f(\Theta_D/T)$ being the integral in Eq. (5). We define ρ_r and $\rho_i(1)$ as the inherent residual and intrinsic resistivities, the latter at $t = 1$. It is then appropriate to replace σ_{dc} in Eq. (4) below T_c by

$$\sigma_{dc}(t) \Rightarrow \frac{n_n(t)}{n} \frac{1}{\rho_r + \rho_i(1)t^5 g(t)} = \frac{n_n(t)e^2 \tau(t)}{m}. \quad (8)$$

We define a resistivity ratio $r = \rho_r/\rho_i(1)$ with $1/\rho_i(1) = \sigma_i(1) = \sigma_{dc}(T_c)(r+1)$. The electron scattering time follows from Eq. (8),

$$\tau(t) = \frac{\mu_0 \lambda^2(0) \sigma_{dc}(T_c)(r+1)}{r + t^5 g(t)}, \quad (9)$$

and the conductivity $\sigma = \sigma' - i\sigma''$ below T_c is

$$\sigma'(t) = \sigma_{dc}(T_c) \left(\frac{n_n(t)/n}{r + t^5 g(t)} \right) \frac{r+1}{1 + [\omega\tau(t)]^2}, \quad (10)$$

$$\sigma''(t) = [\omega\mu_0 \lambda^2(t)]^{-1} + \omega\tau(t)\sigma'(t). \quad (11)$$

The term $[\omega\mu_0 \lambda^2(t)]^{-1} = n_s(t)e^2/m\omega$ arises from the superelectrons³⁴ and is the dominant term in Eq. (11) at low temperatures provided $\omega\tau < 1$. When $s = (\sigma'/\sigma'')^2 \ll 1$, Eq. (1) reduces to

$$R_s \approx \frac{1}{2} \sqrt{\omega\mu_0} \frac{\sigma'}{(\sigma'')^{3/2}}. \quad (12)$$

The latter equation is often used to interpret experimental results. In order to calculate R_s from Eq. (1) or (12) as a function of temperature, $\lambda(t)$ and other parameters have to be known. Measurements shown in Fig. 3 of Hosseini *et al.*²¹ display the temperature dependence of $[\lambda(0)/\lambda(t)]^2$ in the ab plane with currents parallel to the a direction of

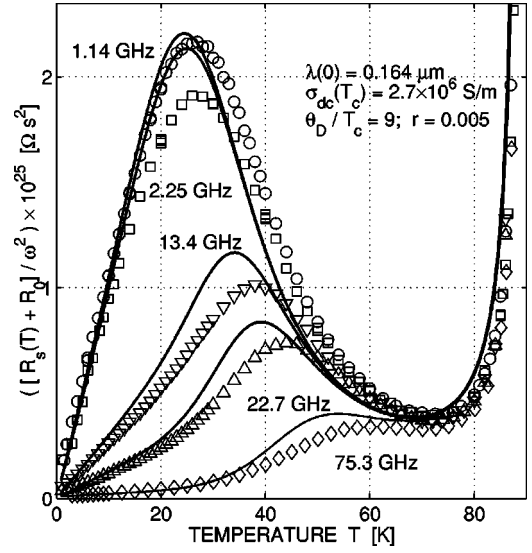


FIG. 2. Linear plot of resistance $R_s(T)/\omega^2$ as a function of temperature for five experimental frequencies calculated from Eq. (1). The experimental points are from Ref. 21, Fig. 2. We put $R_0 = 0.2$ m Ω for 75.3 GHz, zero for all other frequencies.

YBa₂Cu₃O_{7- δ} . The author fitted the latter data²¹ with $a = 0.471$ to the following approximate equation, shown in Fig. 1:

$$[\lambda(0)/\lambda(t)]^2 \approx 1 - at - (1-a)t^6. \quad (13)$$

The slope of R_s in the ab plane as $T \rightarrow 0$ K is

$$\frac{dR_s}{dT} = \frac{1}{2} \frac{\omega^2 \mu_0^2}{T_c} \frac{a}{r} \frac{\lambda^3(0) \sigma_{dc}(T_c)(r+1)}{1 + [\omega\tau(0)]^2}, \quad (14)$$

and $n_n(t)/n = at + (1-a)t^6$ in Eq. (10). It should be remembered that Eq. (13) is empirical and $n_n(t)/n$ is probably sample dependent to a certain degree.

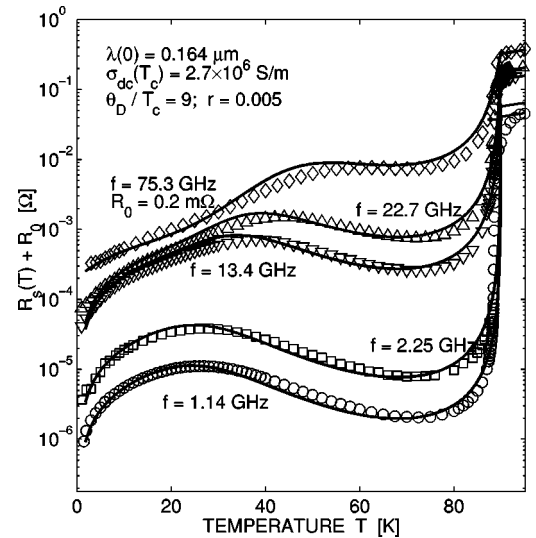


FIG. 3. Semilogarithmic plot of resistance $R_s(T)$ as a function of temperature for 1.14, 2.25, 13.4, 22.7, and 75.3 GHz with $R_0 = 0$ for all frequencies except for 75.3 GHz. R_s is calculated from Eq. (1). The points are from Ref. 21, Fig. 1. The experimental R_s value, extrapolated to 0 K, is 0.2 m Ω at 75.3 GHz.

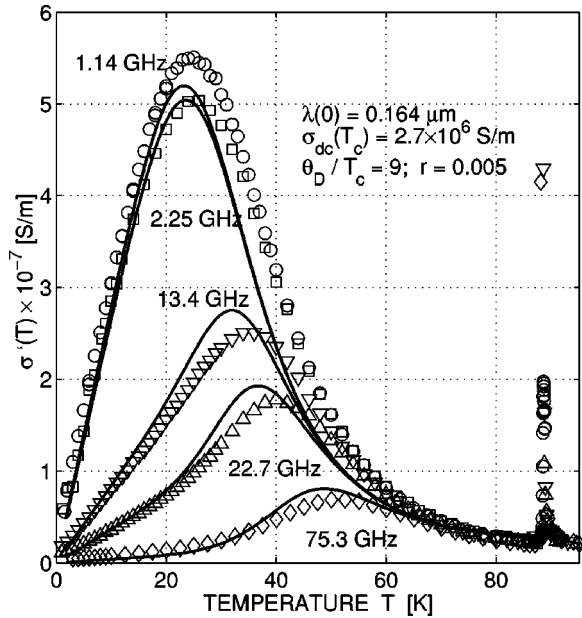


FIG. 4. Linear plot of the real part of the conductivity σ' as a function of temperature, calculated from Eq. (10) for the five experimental frequencies. The points are from Fig. 4 of Ref. 21 and where obtained courtesy of the Vancouver group (D. A. Bonn).

Equations (14) and (10) show that R_s and σ' increase linearly with t at low temperatures and the slopes are proportional to $a(1+1/r)$, provided that $[\omega\tau(0)]^2 \ll 1$. This is a consequence of the linear increase of the quasiparticles with temperature near absolute zero. However, if $[\omega\tau(0)]^2 \gg 1$, the slope of R_s near 0 K is proportional to $a/(1+1/r)$ which changes considerably the slope of R_s and σ' with frequency. This important feature distinguishes $\text{YBa}_2\text{Cu}_3\text{O}_{7-\delta}$ from classical low-temperature superconductors. Equation (10) is also valid for $t > 1$ if one realizes that above T_c the term $n_n(t)/n$ in Eq. (10) has to be replaced by 1. Equation (9) is valid above and below T_c , and R_s can be calculated readily from Eq. (1) with $n_s(t) \neq 0$ below T_c and $n_s = 0$ above T_c . The slopes of R_s and of σ' are discontinuous at T_c , neglecting fluctuation effects.^{35–38}

The rf skin depth δ is

$$\delta = [\mu_0 \pi f \sigma'' (\sqrt{1+s} + 1)]^{-1/2}. \quad (15)$$

Over most of the superconducting temperature interval below T_c the value of $s \ll 1$ and, consequently, $\delta(t) \approx \lambda(t)$. Above T_c , provided that the value of $s \gg 1$, the skin depth $\delta = (\mu_0 \pi f \sigma')^{-1/2}$.

The following results were calculated from Eq. (1) with Eqs. (9)–(11) with $T_c = 90$ K, $\Theta_D = 9T_c$, $\sigma_{dc}(T_c) = 2.7 \times 10^6$ S/m, $r = \rho_r/\rho_i(T_c) = 0.005$, and $\lambda(0) = 0.164$ μm . The $\sigma_{dc}(T_c)$ value was estimated from the conductivity data, Fig. 4, of Hosseini *et al.*²¹ near T_c . From the low-frequency slope of R_s at low temperatures, Eq. (14), the ratio $\lambda^3(0)/r$ is estimated. The Θ_D value is consistent with Ref. 39. The r value should be interpreted as a relative measure of electron scattering attributed to the impurity content. Although the crystal was cleaved and smaller pieces were used at the higher frequencies, the same parameters for all frequencies and temperatures were used in order to see whether or not consistent frequency and temperature patterns emerge.

One can see from Fig. 1 of the Vancouver data²¹ (present Fig. 3) that when R_s is extrapolated to 0 K for the 75.3 GHz data, a finite resistance R_0 is obtained. This resistance is different in nature from the residual resistivity denoted here by ρ_r . It is not clear what the origin of R_0 is except that its imprint on the measurements is different from that of the residual resistivity ρ_r . Perhaps a small number of extraneous impurity carriers remained near $T=0$ K, or perhaps a universal conductivity limit is reached as $T \rightarrow 0$ K.²⁴ We neglect in the following figures R_0 for $\text{YBa}_2\text{Cu}_3\text{O}_{7-\delta}$, except for the 75.3 GHz experimental data which we interpreted as being $R_s(T) + R_0$ with $R_0 \approx 0.2$ m Ω .

Figure 2 shows a linear plot of $R_s(T)/\omega^2$ with the above chosen values of $\lambda(0)$, T_c , Θ_D , r , and $\sigma_{dc}(T_c)$ for five experimental frequencies. The experimental points are from Fig. 2 of Hosseini *et al.*²¹ and the $R_s(T)$ values are calculated from Eq. (1) with Eqs. (9)–(11). There is a pronounced peak at the lower temperatures, in particular for the lower frequencies. By dividing by ω^2 , the contribution of R_0 to the 75.3 GHz data becomes insignificant in the latter figure.

Figure 3 is a semilogarithmic plot of $R_s(T)$, corresponding to Fig. 1 of Hosseini *et al.*²¹ with the same frequencies as shown in the above figure. The theoretical curves are calculated from Eq. (1) with Eqs. (9)–(11), neglecting R_0 except for 75.3 GHz. The fit at high frequencies (75.3 GHz) is considerably better when $R_0 \approx 0.2$ m Ω is added to $R_s(T)$. Near T_c the resistance changes by several orders of magnitude, in particular for the lower frequencies, has a discontinuity in the slope at T_c , and increases quasilinearly above T_c . The discontinuity is caused by assuming that only normal electrons exist above T_c , while the experimental data show a “rounding,” probably due to fluctuations,^{35,36} foreshadowing the superconducting state. The agreement of the calculations with the experiments is very good overall, above and below T_c .

Figure 4 shows the real part of the conductivity $\sigma'(T)$ calculated from Eq. (10). The experimentally extracted points are from Fig. 4 of Hosseini *et al.*²¹ and were calculated by the Vancouver group using their Eq. (3.5). The $1 + (\omega\tau)^2$ term is responsible for depressing σ' at higher frequencies and shifting the maximum to higher temperatures. The slope of σ' is discontinuous at T_c . This discontinuity is not related to the peak in σ' some experimenters obtain^{1,15,21,36} when extracting σ' from R_s measurements near T_c .

Figure 5 is the conductivity spectrum calculated from Eq. (10) with Eq. (9) for various constant temperatures with the above-stated parameters. As found by Hosseini *et al.*,²¹ below 25 K the spectrum is approximately Drude-like for the thermally excited quasiparticles with a narrow peak at low frequencies, corresponding to a low-pass filter. Figure 5 should be compared with Figs. 5 and 6 of Ref. 21. From such a plot Hosseini *et al.*²¹ extracted the scattering rate $1/\tau(T)$ which is shown in Fig. 6 and is compared to that calculated from Eq. (9) with the above parameters. Below 25 K the numerical values agree very closely. Above 25 K they deviate slightly (probably within experimental error). However, the overall shape is very similar. At this point it should be mentioned that a T^n dependence of $1/\tau(T)$ with n between 4 and 5 was proposed previously by Yu *et al.*⁴⁰ and also a

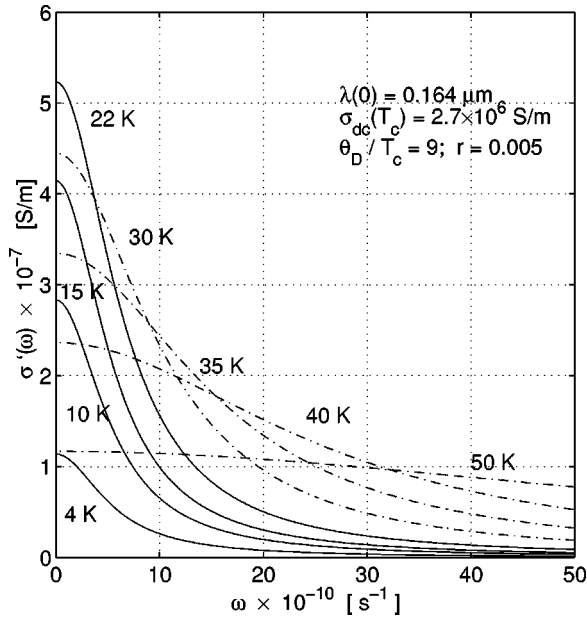


FIG. 5. Conductivity spectrum calculated from Eq. (10) for various fixed temperatures. Compare this plot to Figs. 5 and 6 of Ref. 21.

$r + t^5$ dependence by Trunin *et al.*¹⁵ The latter (not shown) is in between the two plotted curves.

The scattering rate $1/\tau(T)$, Eq. (9), consists of two terms, a temperature independent term, controlled by the residual electron scattering rate, and a term controlled by a temperature dependent scattering rate. Cleaner specimens (smaller r values) have a smaller scattering rate than dirtier specimens (larger damping term).²² Below 20 K all values of $\tau(r)$ are practically temperature independent for all reasonable r values, since in this temperature range $r \gg t^5 g(t)$. In particular, we find for $r = 0.005$, no noteworthy variation below 22 K. This, however, contradicts the results shown in Fig. 8 of Ref.

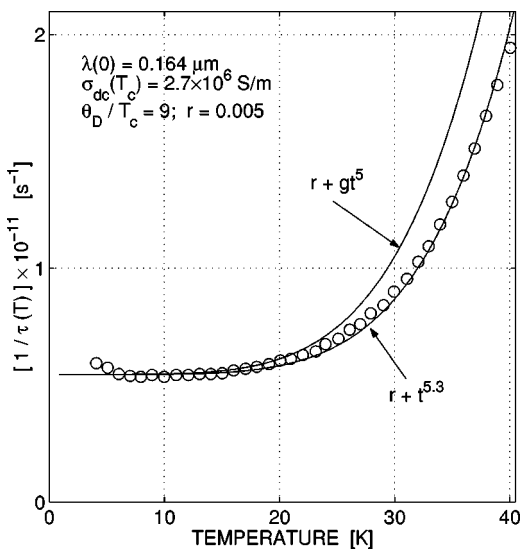


FIG. 6. Scattering rate of the quasiparticles corresponding to the conductivity spectrum of above figure calculated from Eq. (9) with $r + gt^5$ and the latter term replaced by $r + t^{5.3}$. The $r + t^5$ curve (not shown) is in between the two plotted curves. The experimental points are from Fig. 8 of Ref. 21.

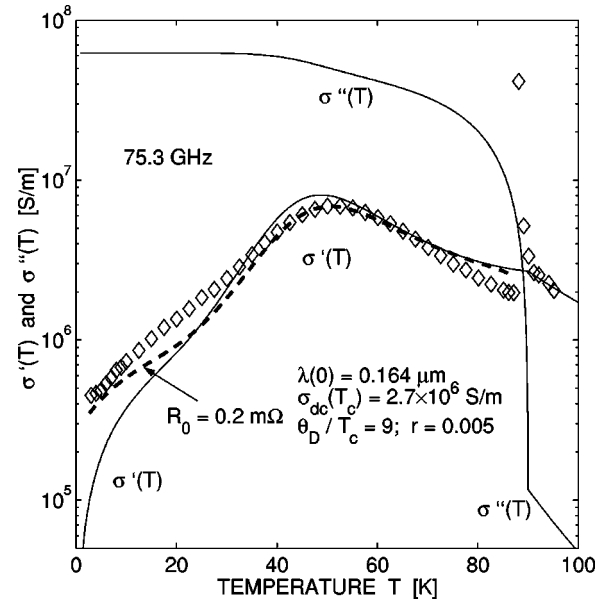


FIG. 7. Real and imaginary parts of the conductivity, σ' and σ'' , as a function of temperature at 75.3 GHz. The dashed line is obtained from Eq. (16) with $R_0 = 0.2$ m Ω . The experimental points are those shown in Fig. 4 obtained from the Vancouver group.

25 which include temperature dependent scattering terms. These cause $1/\tau(t)$ to increase as one goes to lower temperature at the low-temperature end. Since $\tau(T)$ is not measured directly, but extracted from the conductivity spectrum, which in turn has been obtained from $\sigma'(T)$, which is based on direct measurements of the real part of the surface impedance R_s , this discrepancy remains an open question. However, the observed functional behavior of $1/\tau(T)$ is justified theoretically²² by Matthiessen's rule. A consequence of the latter result is that the real part of the conductivity $\sigma'(T)$ varies as T at low temperatures, while the result of Ref. 25 leads to a T^2 dependence at low temperatures.

The solid lines in Fig. 7 are semilogarithmic plots of $\sigma'(T)$ and $\sigma''(T)$, calculated from Eqs. (10) and (11) at 75.3 GHz. When using Eq. (12) to calculate $\sigma'(T)$ at 75.3 GHz, the measured resistance has to be interpreted as the sum of $R_s(T) + R_0$. It then follows from Eq. (12) that

$$\sigma'(T) = \frac{2(R_s(T) + R_0)}{(\omega\mu_0)^2\lambda^3(T)}. \quad (16)$$

The dashed line in Fig. 7 is $\sigma'(T)$ calculated from Eq. (16) and the experimental points are those shown also in Fig. 4. It is obvious that the latter do not represent the true real part of the intrinsic conductivity. For the experiments²¹ on $\text{YBa}_2\text{Cu}_3\text{O}_{7-\delta}$ the deviation of the measured from the true $\sigma'(T)$ at 75.3 GHz is relatively small, but for $\text{Bi}_2\text{Sr}_2\text{CaCu}_2\text{O}_8$ (Refs. 41–43) and $\text{Tl}_2\text{Ba}_2\text{CuO}_{6+\delta}$ (Ref. 44) the deviations from the true $\sigma'(T)$ are quite appreciable. Since $\omega\tau(0) = 8.7$ at 75.3 GHz, the contribution of the term $\omega\tau(T)\sigma'(T)$ to $\sigma''(T)$ [Eq. (11)] is appreciably below 46 K and cannot be completely ignored.

Figure 8 shows a linear plot of R_s and X_s at 75.3 GHz for temperatures above 80 K, and Fig. 9 shows $R_s(T)$ below 80 K. The reactance X_s is calculated from Eq. (2) with Eqs. (9)–(11). X_s has a peak just below T_c , more noticeable for

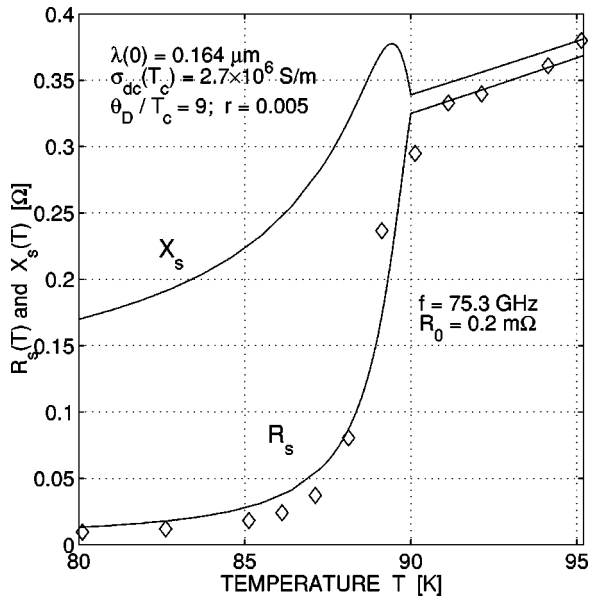


FIG. 8. Reactance $X_s(T)$ and resistance $R_s(T)$ near T_c for 75.3 GHz. The experimental data are from the Vancouver group. Note the peak in $X_s(T)$ below T_c and the splitting of $X_s(T)$ and $R_s(T)$ above T_c .

the higher frequencies, and is split from R_s above T_c . When the conduction current is dominant over the displacement current one usually assumes that $R_s = X_s$. However, it follows from Eqs. (1) and (2) that above T_c

$$\frac{X_s}{R_s} \approx \sqrt{\frac{1 + \omega\tau(T)}{1 - \omega\tau(T)}}. \quad (17)$$

Although above T_c the value of $\omega\tau \ll 1$ for $f < 100$ GHz, it is not necessarily true that $\omega\tau$ can be completely neglected. A consequence is that $R_s \neq X_s$ above T_c , as is observed by experiments³⁶ on $\text{Tl}_2\text{Ba}_2\text{CuO}_{6+\delta}$. For the experi-

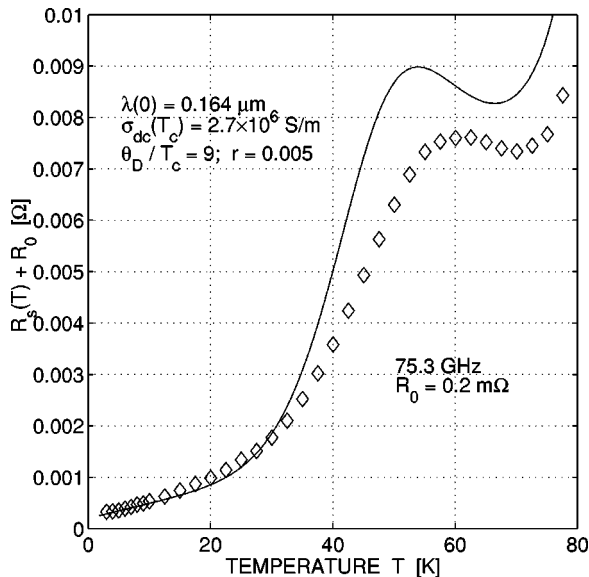


FIG. 9. Resistance $R_s(T)$ below 80 K at 75.3 GHz. The experimental data are from the Vancouver group. Note the offset resistance R_0 , the slope of $R_s(T)$ at low temperatures, and the small difference in $R_s(T)$ between the peak and the valley.

ments under consideration²¹ $\omega\tau < 1$ for 1.14 and 2.25 GHz at all temperatures, while for 13.4, 22.7, and 75.3 GHz, $\omega\tau < 1$ above 27, 33.5, and 45.8 K, respectively, while at lower temperatures $\omega\tau > 1$.

Figure 9 is a linear plot of $R_s(T)$ at 75.3 GHz below 80 K. The experimental points are from the Vancouver group. The large peak and valley which exist at low frequencies disappear at the higher frequencies and approach an inflection point with a horizontal tangent near but above 75.3 GHz. For higher frequencies the inflection point with the horizontal tangent disappears completely and $R_s(T)$ should show a resistive transition which is similar (although not the same) to those which are observed on heavily doped specimens at lower frequencies.³

We find the following: At low temperatures the normal state dc resistivity varies approximately as T^5 . This is also the dominant temperature term controlling $1/\tau(T)$, R_s , and $\sigma'(T)$ of $\text{YBa}_2\text{Cu}_3\text{O}_{7-\delta}$ at the low-temperature end. We assume that the residual scattering rate due to ρ_r is constant over the whole temperature interval. From the good agreement of the primary experimental data²¹ with the present model calculations, shown in Figs. 2–4, obtained from Eq. (1) with Eqs. (9)–(11), this assumption appears to be correct, at least to first order, indicating that electron-phonon interactions are an important mechanism in high- T_c superconductors, at least that part of the mechanism which relates to the quasiparticle part of the electron fluid. We carried over unchanged the normal state scattering rate [Eq. (9)] into the superconducting state as T is decreased through T_c . This is not in conflict with the surface resistance experiments. There is a sharp discontinuity of the theoretical slope of R_s and σ' at T_c without introducing an abrupt change in $\tau(T)$ at T_c (see Figs. 7 and 8).

In conclusion, we have tested a model^{16,22} which describes correctly the essential features and numerical values of the microwave surface resistance measurements²¹ of $\text{YBa}_2\text{Cu}_3\text{O}_{7-\delta}$. The R_0 value obtained from the extrapolated experimental data is subtracted from the measured $R_{\text{expt}}(T)$ data in order to obtain the intrinsic $R_s(T)$ value. Except for the 75.3 GHz results, the contribution of R_0 to R_{expt} was neglected. Increasing the residual resistivity (the resistivity ratio r) decreases the slope of R_s at the low-temperature end at low frequencies and reduces the microwave losses of $\text{YBa}_2\text{Cu}_3\text{O}_{7-\delta}$. At low temperatures, R_s increases linearly with temperature due to a linear change of $[\lambda(t)]^{-2}$ with temperature and a constant electron scattering rate. The empirical temperature dependence of $[\lambda(t)]^{-2}$, which is used here, is distinct from the empirical $1-t^4$ dependence, usually accepted for classical superconductors. Equation (13) is a fit to the observed $\lambda(t)$ which is justified as being due to d -wave^{24,26} superconductivity. The maximum of $\sigma'(t)$ is caused by an effective Grüneisen temperature dependent electron scattering rate, a gradual freezing out of the quasiparticles, and a remaining residual resistivity ρ_r as $T \rightarrow 0$ K. The peak of $\sigma'(t)$ of a clean specimen of $\text{YBa}_2\text{Cu}_3\text{O}_{7-\delta}$ is decreased and shifted to higher temperatures when the frequency and the residual resistivity are independently increased. New theoretical investigations of possible scattering mechanisms below 20 K within the framework of d -wave models have been initiated very recently.^{45,46}

The present two-fluid analysis is limited to the experi-

ments of Ref. 21. A global analysis of other experiments on YBCO (Ref. 18) and other cuprates^{16,41,42,44} is in preparation.⁴⁷ Hopefully, the present and future⁴⁷ analyses will be a helpful guide for investigations of high- T_c superconductors from a microscopic point of view. Topics which require further investigations are the temperature dependence of $\lambda(T)$ of high- T_c superconductors, an explanation of

whether the extrapolated resistance $R_0(\omega)$ is of fundamental nature or not, and an investigation of $\tau(T)$ near and above T_c .

The author thanks D. A. Bonn for permission to use the original data points of the Vancouver group in the figures and M. R. Trunin for very constructive suggestions and discussions.

- ¹D. A. Bonn and W. N. Hardy, in *Physical Properties of High Temperature Superconductors*, edited by Donald M. Ginsberg (World Scientific, Singapore, 1996), Vol. VI, pp. 7–97.
- ²K. Zhang, D. A. Bonn, S. Kamal, R. Liang, D. J. Baar, W. N. Hardy, D. Basov, and T. Timusk, Phys. Rev. Lett. **73**, 2484 (1994).
- ³D. A. Bonn, S. Kamal, K. Zhang, R. Liang, D. J. Baar, E. Klein, and W. N. Hardy, Phys. Rev. B **50**, 4051 (1994).
- ⁴W. N. Hardy, D. A. Bonn, D. C. Morgan, R. Liang, and K. Zhang, Phys. Rev. Lett. **70**, 3999 (1993).
- ⁵D. A. Bonn, P. Dosanjh, R. Liang, and W. N. Hardy, Phys. Rev. Lett. **68**, 2390 (1992).
- ⁶D. A. Bonn, R. Liang, T. M. Riseman, D. J. Baar, D. C. Morgan, K. Zhang, P. Dosanjh, T. L. Duty, A. MacFarlane, G. D. Morris, J. H. Brewer, W. N. Hardy, C. Kallin, and A. J. Berlinsky, Phys. Rev. B **47**, 11 314 (1993).
- ⁷D. A. Bonn, S. Kamal, Kuan Zhang, Ruixing Liang, and W. N. Hardy, J. Phys. Chem. Solids **56**, 1941 (1995).
- ⁸D. A. Bonn, S. Kamal, A. Bonakdarpour, R. Liang, W. N. Hardy, C. C. Homes, D. N. Basov, and T. Timusk, Czech. J. Phys. **46**, 3195 (1996).
- ⁹S. Kamal, Ruixing Liang, A. Hosseini, D. A. Bonn, and W. N. Hardy, Phys. Rev. B **58**, 8933 (1998).
- ¹⁰A. Hosseini, Saeid Kamal, D. A. Bonn, Ruixing Liang, and W. N. Hardy, Phys. Rev. Lett. **81**, 1298 (1998).
- ¹¹M. C. Nuss, P. M. Mankiewich, M. L. O'Malley, E. H. Westerwick, and P. B. Littlewood, Phys. Rev. Lett. **66**, 3305 (1991).
- ¹²U. Dähne, Y. Goncharov, N. Klein, N. Tellemann, G. Kozlov, and K. Urban, J. Supercond. **8**, 129 (1995).
- ¹³K. Krishana, J. M. Harris, and N. P. Ong, Phys. Rev. Lett. **75**, 3529 (1995).
- ¹⁴M. R. Trunin, A. A. Zhukov, and A. T. Sokolov, J. Phys. Chem. Solids **59**, 2125 (1998).
- ¹⁵M. R. Trunin, J. Supercond. **11**, 381 (1998).
- ¹⁶M. R. Trunin, A. A. Zhukov, G. A. Emel'chenko, and I. G. Naumenko, Pis'ma Zh. Éksp. Teor. Fiz. **65**, 893 (1997) [JETP Lett. **65**, 938 (1997)].
- ¹⁷M. R. Trunin, Phys. Usp. **41**, 843 (1998).
- ¹⁸H. Srikanth, B. A. Willemsen, T. Jacobs, S. Sridhar, A. Erb, E. Walker, and R. Flükiger, Phys. Rev. B **55**, R14 733 (1997).
- ¹⁹C. T. Rieck, K. Scharnberg, S. Hensen, and G. Müller, J. Low Temp. Phys. **105**, 503 (1996).
- ²⁰S. Hensen, G. Müller, C. T. Rieck, and K. Scharnberg, Phys. Rev. B **56**, 6237 (1997).
- ²¹A. Hosseini, Saeid Kamal, P. Dosanjh, J. Preston, Ruixing Liang, W. N. Hardy, and D. A. Bonn, Phys. Rev. B **60**, 1349 (1999).
- ²²H. J. Fink, Phys. Rev. B **58**, 9415 (1998).
- ²³J. Annett, N. Goldenfeld, and S. R. Renn, Phys. Rev. B **43**, 2778 (1991).
- ²⁴P. A. Lee, Phys. Rev. Lett. **71**, 1887 (1993).
- ²⁵P. J. Hirschfeld, W. O. Puttka, and D. J. Scalapino, Phys. Rev. B **50**, 10 250 (1994).
- ²⁶P. J. Hirschfeld and N. Goldenfeld, Phys. Rev. B **48**, 4219 (1993).
- ²⁷S. Chakravarty, A. Sudbø, Ph.W. Anderson, and S. Strong, Science **261**, 337 (1993).
- ²⁸R. A. Klemm and S. H. Liu, Phys. Rev. Lett. **74**, 2343 (1995).
- ²⁹D. Djajaputra and J. Ruvalds, Phys. Rev. B **55**, 14 148 (1997); C. T. Rieck, K. Scharnberg, and J. Ruvalds, *ibid.* **60**, 12 432 (1999).
- ³⁰C. T. Rieck, W. A. Little, J. Ruvalds, and A. Virosztek, Phys. Rev. B **51**, 3772 (1995).
- ³¹J. R. Waldram, P. Theopistou, A. Porch, and H.-M. Cheah, Phys. Rev. B **55**, 3222 (1997).
- ³²A. A. Abrikosov, *Fundamentals of the Theory of Metals* (North-Holland, Amsterdam, 1988), p. 49.
- ³³E. Grüneisen, Ann. Phys. (Leipzig) **16**, 530 (1933).
- ³⁴T. Van Duzer and C. W. Turner, *Principles of Superconductive Devices and Circuits* (Elsevier, New York, 1981), p. 126.
- ³⁵L. G. Aslamasov and A. I. Larkin, Phys. Lett. **26A**, 238 (1968).
- ³⁶J. R. Waldram, D. M. Broun, D. C. Morgan, R. Ormeno, and A. Porch, Phys. Rev. B **59**, 1528 (1999).
- ³⁷S. M. Anlage, J. Mao, J. C. Booth, Dong Ho Wu, and J. L. Peng, Phys. Rev. B **53**, 2792 (1996).
- ³⁸J. C. Booth, Dong Ho Wu, S. B. Qadri, E. F. Skeleton, M. S. Osofsky, A. Piqué, and S. M. Anlage, Phys. Rev. Lett. **77**, 4438 (1996).
- ³⁹R. Aoki, K. Sakai, H. Murakami, T. Nakamura, H. Kawaji, and M. Itoh, Physica C **185–189**, 1065 (1991).
- ⁴⁰R. C. Yu, M. B. Salamon, Jian Ping Lu, and W. C. Lee, Phys. Rev. Lett. **69**, 1431 (1992).
- ⁴¹S.-F. Lee, D. C. Morgan, R. J. Ormeno, D. M. Broun, R. A. Doyle, J. R. Waldram, and K. Kadowaki, Phys. Rev. Lett. **77**, 735 (1996).
- ⁴²T. Jacobs, S. Sridhar, Q. Li, G. D. Gu, and N. Koshizuka, Phys. Rev. Lett. **75**, 4516 (1995).
- ⁴³H. J. Fink and M. R. Trunin, Physica B (to be published).
- ⁴⁴D. M. Broun, D. C. Morgan, R. J. Ormeno, S. F. Lee, A. W. Tyler, A. P. Mackenzie, and J. R. Waldram, Phys. Rev. Lett. **77**, 735 (1996).
- ⁴⁵M. H. Hettler and P. J. Hirschfeld, cond-mat/9907150 (unpublished).
- ⁴⁶A. J. Berlinsky, D. A. Bonn, R. Harris, and C. Kallin, cond-mat/9908159 (unpublished).
- ⁴⁷M. R. Trunin, Yu. A. Nefyodov, and H. J. Fink, cond-mat/9911211 (unpublished).